

Ansys Submission to the 7th AIAA Drag Prediction Workshop

Krishna Zore, Cristhian Aliaga, Jeya Selva, Laith
Zori, Boris Makarov

7th AIAA Drag Prediction Workshop
Chicago, IL USA
25-26 June 2022



Outline

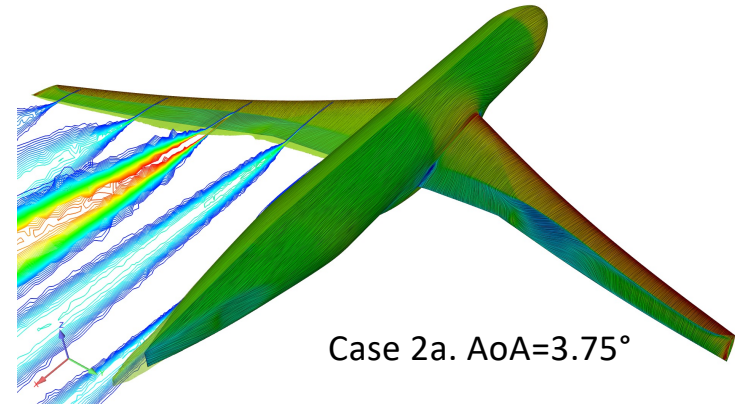
- Goal & Approach
- Introduction to Ansys Fluent-Aero Workspace
- CFD methodology
- CFD results and key observations
 - Case1a: Grid Convergence Study
 - Case2a: Alpha Sweep at Constant Re
 - Case3: Re Sweep at Constant CL
- Summary and Outlook

Goal & Approach

- Goal
 - Predict the effect of shock-induced separation with increasing angle-of-attack at transonic conditions using CFD.
- Approach
 - Use the NASA CRM Wing-Body configuration with prescribed static wing twist and bending, at $M=0.85$:
 - Case 1a: Grid convergence study at constant C_L
 - Case 2a: AoA sweeps at constant Re
 - Case 3: Re sweeps at constant C_L
 - Employ unstructured hybrid grids generated by JAXA to represent the computational domain
 - Use Ansys Fluent Aero to conduct parametric analysis sweeps of AoA and Re at constant C_L and Re .



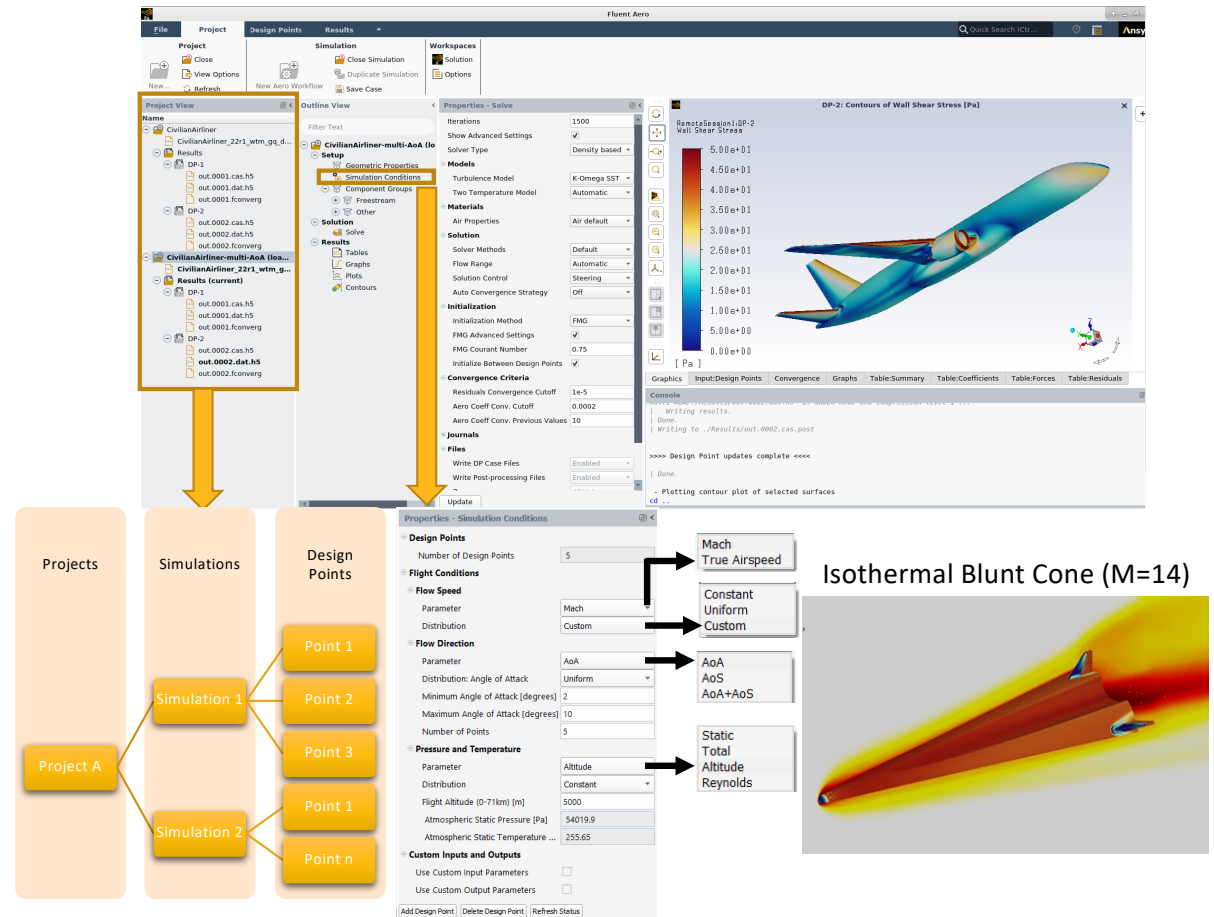
NASA Common Research Model (CRM)



Case 2a. AoA=3.75°

Introduction to Ansys Fluent-Aero Workspace

- Dedicated Fluent Workspace for aerospace external aerodynamics
 - Built inside a Project environment that allows storage and management of multiple simulations
 - Simulations are built from an Outline View UI structure that is similar to Fluent
 - A simulation allows to explore multiple flight and wind tunnel conditions using parametric design point conditions (AoA, Mach, Reynolds, Altitude, etc...), search at constant C_L and post-processing (C_D/C_L , cut plots...)
 - Includes latest solver and convergence advancements tuned for subsonic to hypersonic conditions
 - Released - February 2022

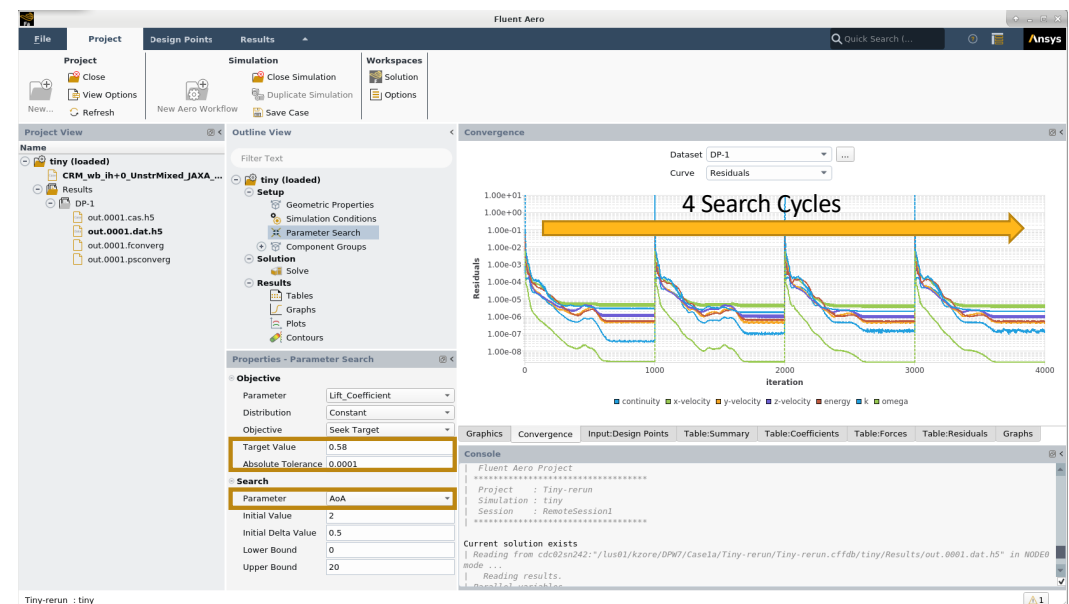


CFD Methodology

- Solver & Properties
 - Steady state RANS simulations.
 - Flow Properties:
 - State: Ideal gas law
 - Specific Heat: Piecewise polynomial (NIST)
 - Thermal Conductivity: Kinetic theory
 - Viscosity: Sutherland's formula
 - Turbulence Properties:
 - Turbulence intensity = 5%
 - Turbulence viscosity ratio = 10
 - Fully Turbulent models:
 - Eddy-viscosity model: k- ω SST (2 equations) – (SST-2003)
 - Simulation Methodology:
 - Pressure based solver with second-order upwind scheme
 - Gradients are evaluated using GGNB known to be robust on skewed and distorted meshes
 - Pseudo Time method is used to achieve convergence

• Parametric Search

- Gradient based secant method to search AoA that meets a target C_L or L for each Design Point



CFD Results

Case1a. Grid Convergence Study:

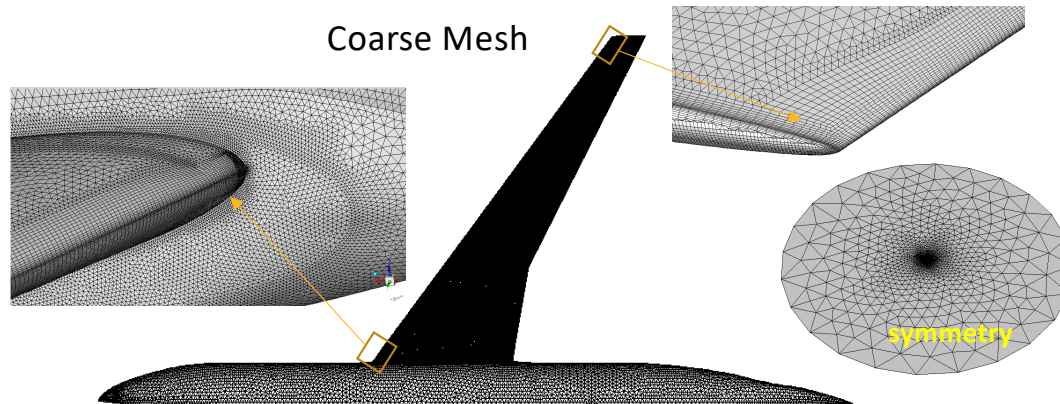
$M = 0.85$; $Re = 20 \text{ million}$; **fixed $CL = 0.58 +/- 0.0001$** ;
Ref. temp. = -250°F ; Baseline LoQ R30 grids



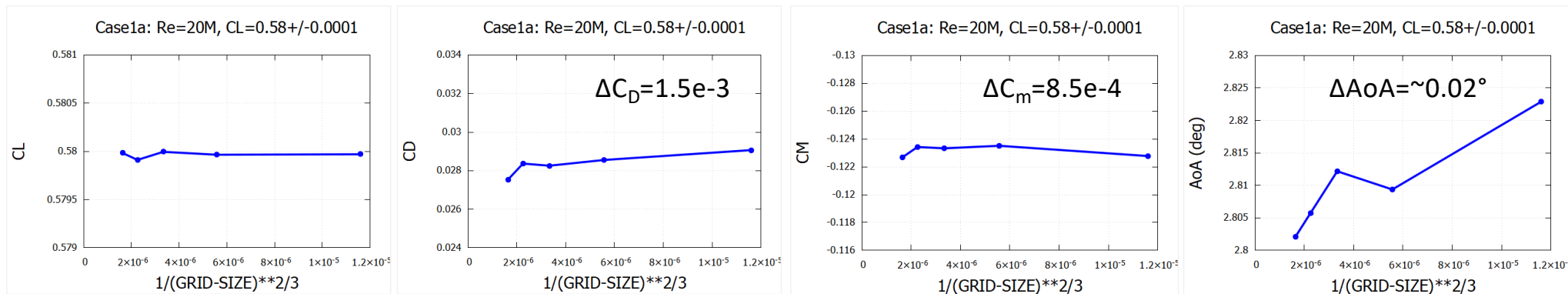
Case 1a: Meshes & Aerodynamic Coefficients

Case1a. Grid Convergence Study: $M = 0.85$; $Re = 20$ million; **fixed CL = 0.58 +/- 0.0001**; Ref. temp. = -250°F; Baseline LoQ R30 grids

JAXA Grid Family (JAXA_Grid.REV00)			
Sr. No	Grid Level	# of Nodes	# of Cells
1	Tiny	8,698,930	25,294,690
2	Coarse	26,891,512	76,058,884
3	Medium	60,184,023	164,065,758
4	Fine	111,843,367	295,240,476
5	Extra Fine	184,127,176	476,358,610



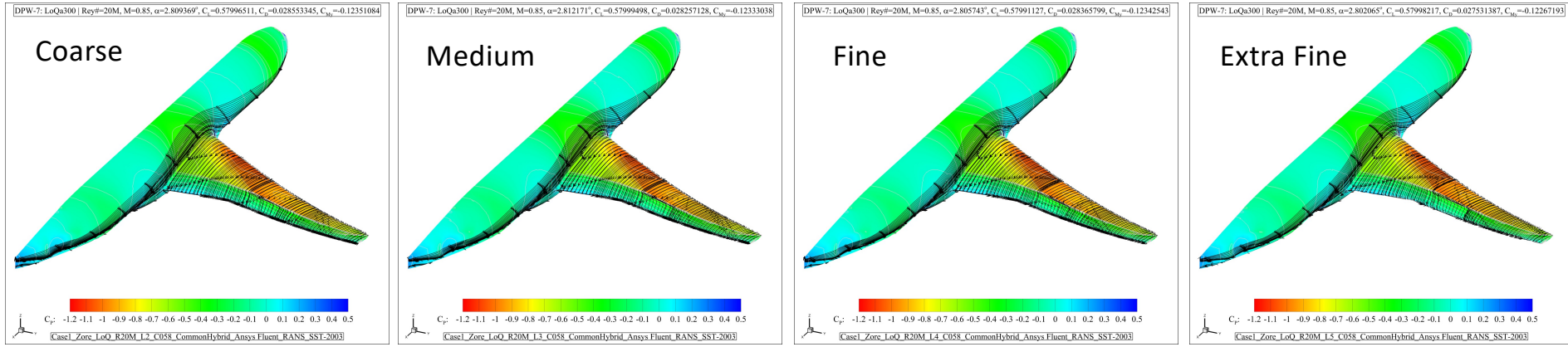
Aerodynamic Coefficient Convergence



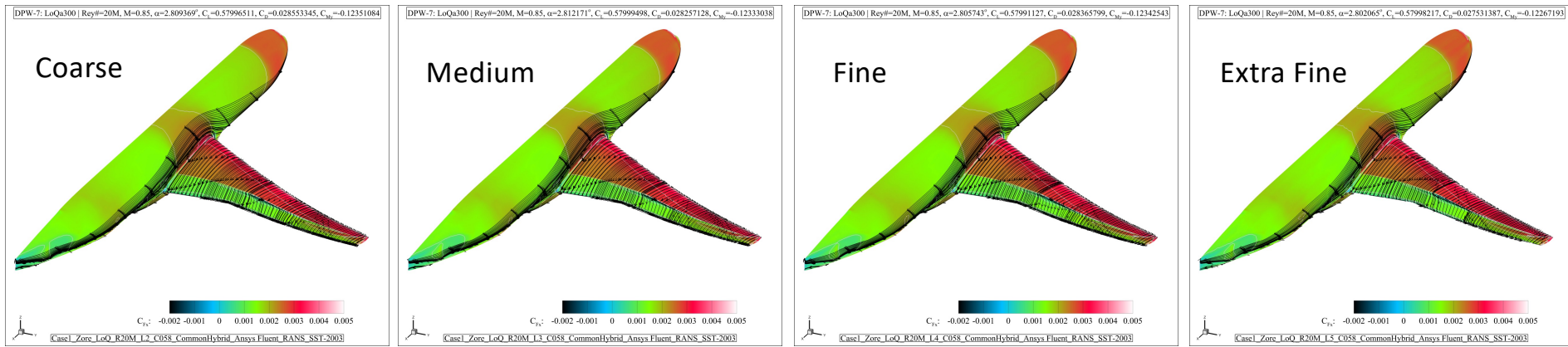
Case 1a: Pressure & Skin Friction Coefficient Contours

Case1a. Grid Convergence Study: $M = 0.85$; $Re = 20 \text{ million}$; **fixed CL = 0.58 +/- 0.0001**; Ref. temp. = -250°F; Baseline LoQ R30 grids

Pressure Coefficient (CP)



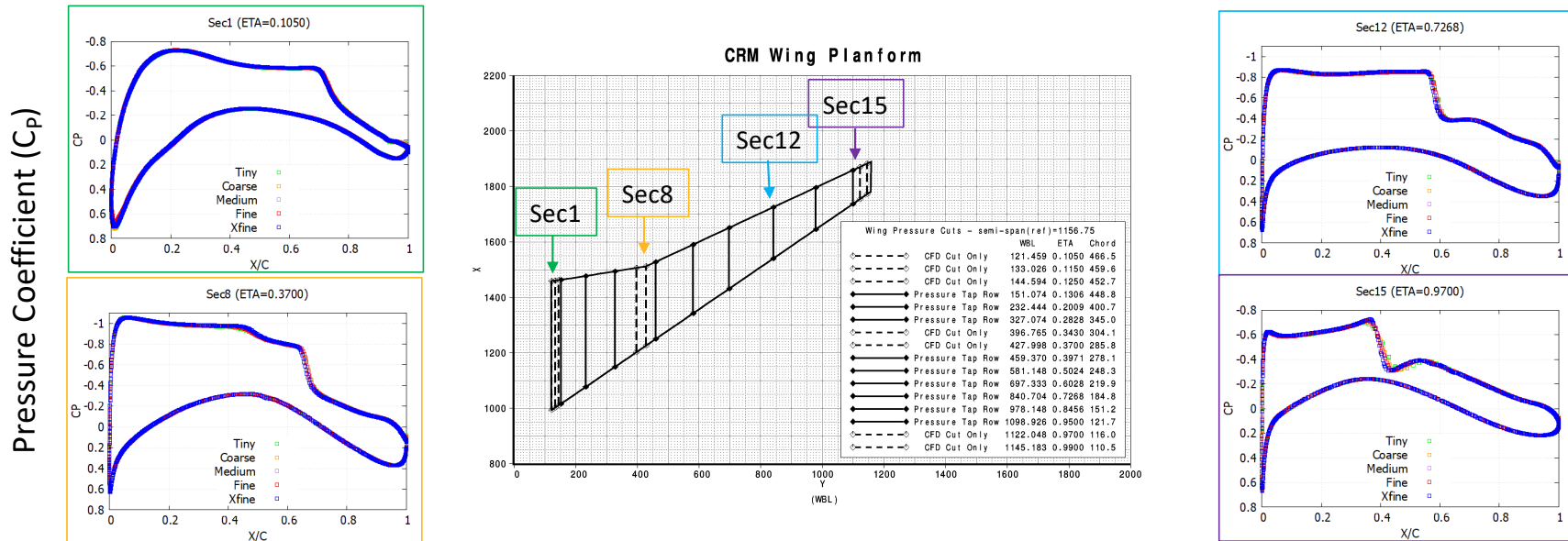
Skin friction Coefficient_x (CFx)



Case 1a: Pressure Coefficients

Case1a. Grid Convergence Study: $M = 0.85$; $Re = 20$ million; **fixed $CL = 0.58 +/- 0.0001$** ; Ref. temp. = -250°F; Baseline LoQ R30 grids

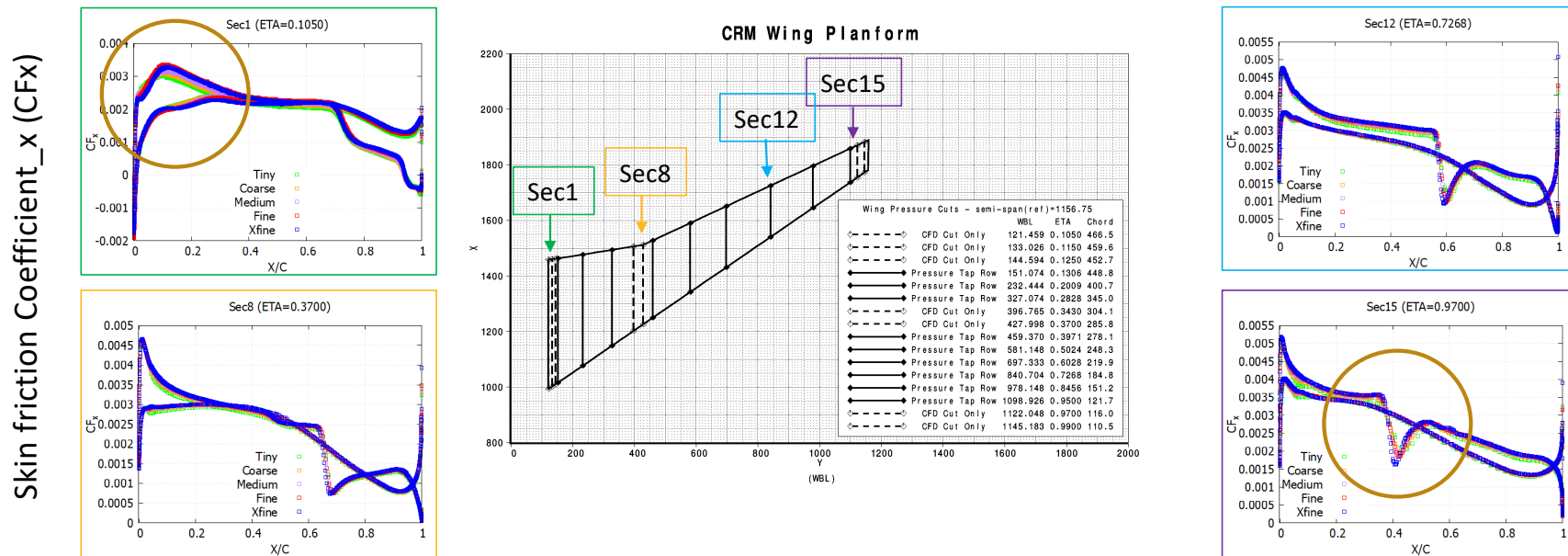
- Observation:
 - All meshes predict very similar pressure distributions over the wing.
 - Some differences are seen at the shock location near wing tip.



Case 1a: Skin Friction Coefficients

Case1a. Grid Convergence Study: $M = 0.85$; $Re = 20$ million; **fixed $CL = 0.58 +/- 0.0001$** ; Ref. temp. = -250°F; Baseline LoQ R30 grids

- Observation:
 - At the wing root, only the Fine and Extra Fine meshes predict similar viscous forces on the suction side.
 - At the wing tip, the location of the shock still changes between the Fine and Extra Fine meshes.



Case 1a: Conclusion

- Grid convergence study using a target C_L with a tolerance of 1e-4 produces slight changes to the AoA (boundary condition).
 - This adds another source of error to the current analysis which can become relevant as the mesh gets finer and can prevent monotonic convergence.
 - **Suggestion:** Perform grid convergence at fix AoA, instead of target C_L , to remove boundary condition uncertainty due to small AoA variations.
- Overall aerodynamic forces over the CRM slightly vary between meshes ($\Delta C_D = \sim 1.5\text{e-}3$ and $\Delta C_m = \sim 8.5\text{e-}4$)
- Viscous distributions revealed that grid independence cannot be guaranteed over the entire wing with the medium mesh.
 - At the wing root, only the Fine and Extra Fine meshes produce similar friction coefficients on the upstream portion of the suction side.
 - At the wing tip, the location of the shock varies between the Fine and Extra Fine meshes.

CFD Results

Case2a. Alpha Sweeps at Constant Re

$M = 0.85$; $Re = 20 \text{ million}$; Ref. temp. = -250°F ; Baseline LoQ R30 grids

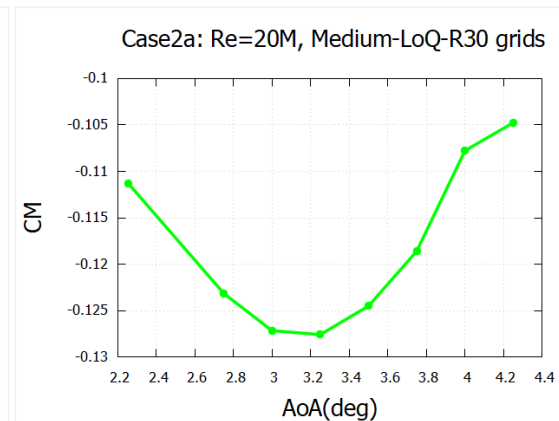
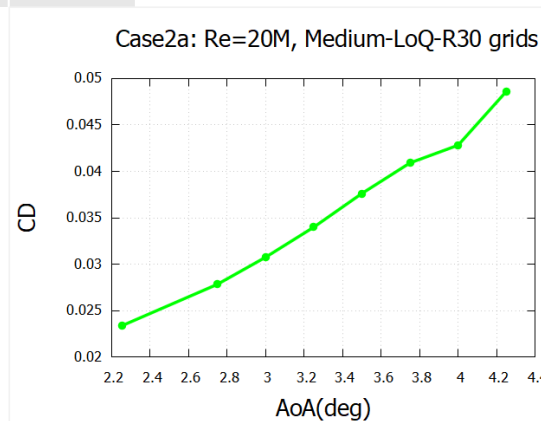
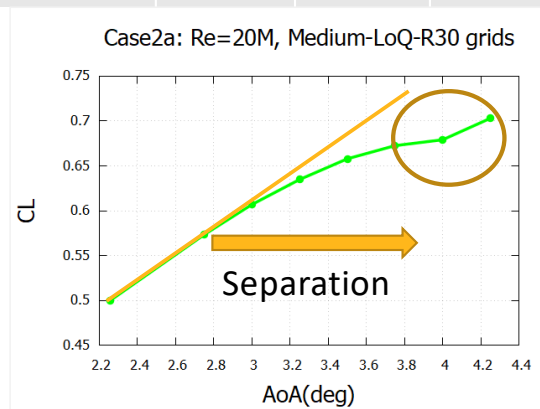
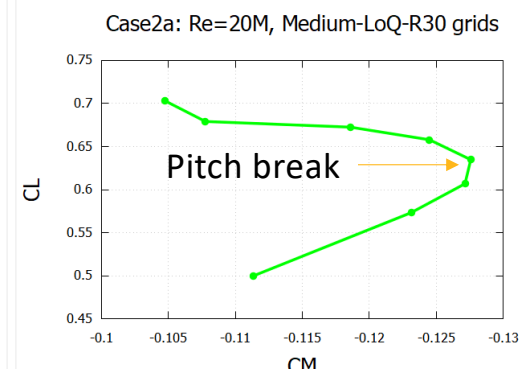
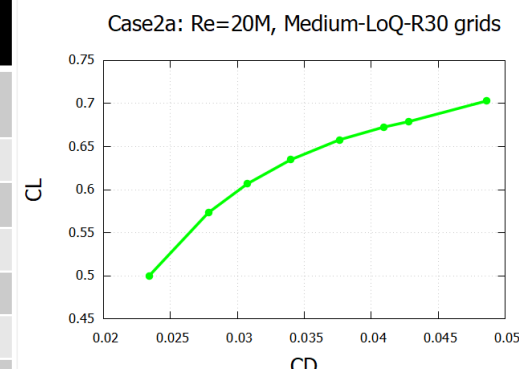
CL = 0.50 2.50-deg LoQ AE CRM geometry
AoA = 2.75° 2.75-deg LoQ AE CRM geometry
AoA = 3.00° 3.00-deg LoQ AE CRM geometry
AoA = 3.25° 3.25-deg LoQ AE CRM geometry
AoA = 3.50° 3.50-deg LoQ AE CRM geometry
AoA = 3.75° 3.75-deg LoQ AE CRM geometry
AoA = 4.00° 4.00-deg LoQ AE CRM geometry
AoA = 4.25° 4.25-deg LoQ AE CRM geometry



Case 2a: Conditions and Aerodynamic Coefficients

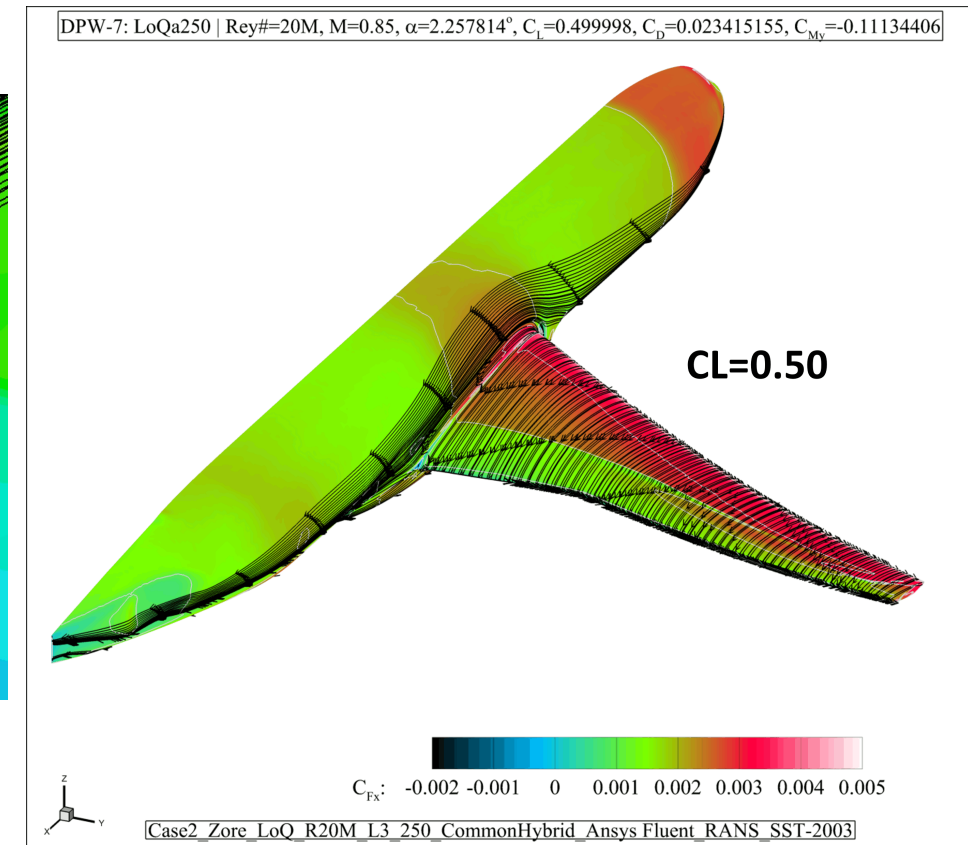
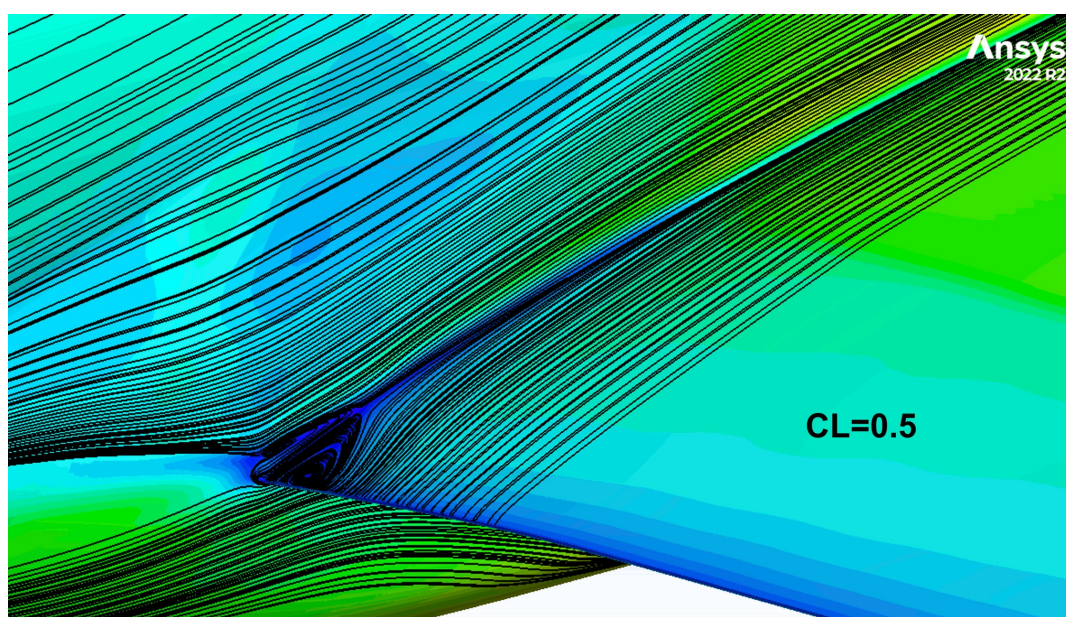
Case2a. Alpha Sweeps at Constant Re: $M = 0.85$; $Re = 20$ million; Ref. temp. = -250°F; Baseline LoQ R30 grids

Grid Level medium	AoA (deg)	CL	CD	CM
2.50-deg LoQ AE CRM geom.	2.2578	0.4999	0.02341	-0.1113
2.75-deg LoQ AE CRM geom.	2.75	0.5734	0.02784	-0.1231
3.00-deg LoQ AE CRM geom.	3	0.6069	0.03075	-0.1271
3.25-deg LoQ AE CRM geom.	3.25	0.6349	0.03399	-0.1275
3.50-deg LoQ AE CRM geom.	3.5	0.6579	0.03762	-0.1244
3.75-deg LoQ AE CRM geom.	3.75	0.6726	0.04091	-0.1186
4.00-deg LoQ AE CRM geom.	4	0.6791	0.04282	-0.1077
4.25-deg LoQ AE CRM geom.	4.25	0.7031	0.04861	-0.1047



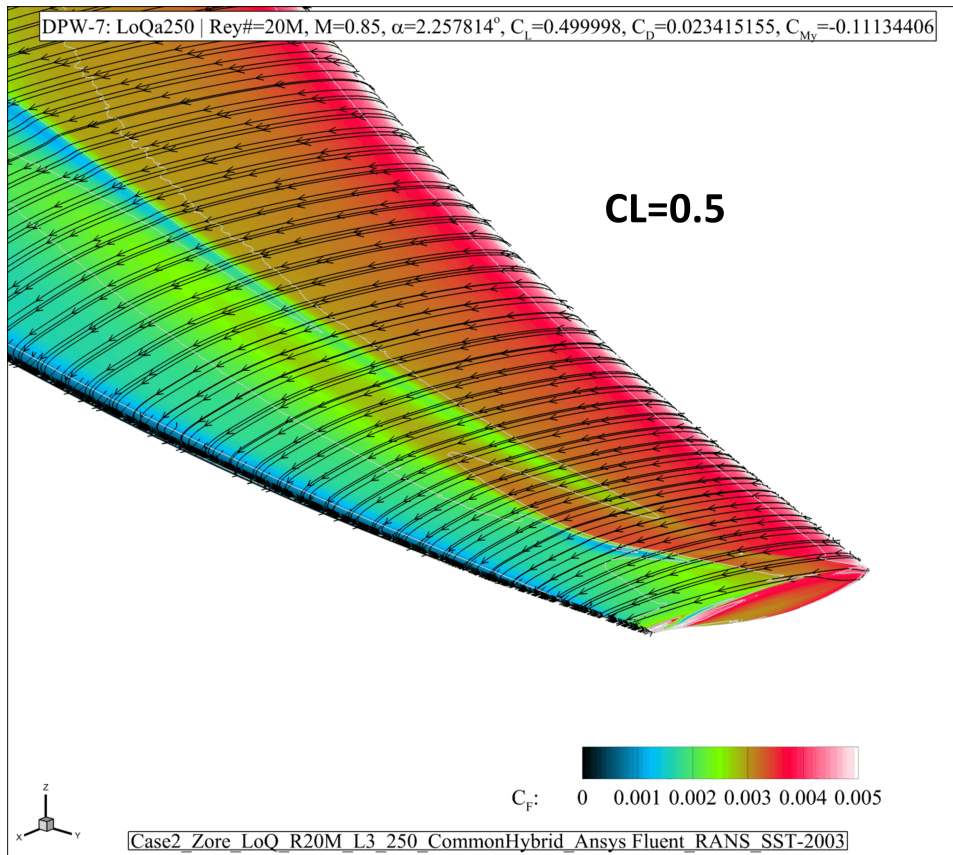
Case 2a: Shear Stress Lines at Wing Root and Mid-Span

Case2a. Alpha Sweeps at Constant Re: $M = 0.85$; $Re = 20$ million; Ref. temp. = -250°F ; Baseline LoQ R30 grids



Case 2a. Shear Stress Lines at Wing Tip

Case2a. Alpha Sweeps at Constant Re: $M = 0.85$; $Re = 20$ million; Ref. temp. = -250°F ; Baseline LoQ R30 grids



- Shear stress lines affected by the growing presence of the separation bubble
- Sudden increase of the separation zone near the wing tip after 4.0°
- Wing bending decreases between 4.0° and 4.25° which could explain the inflection in C_L

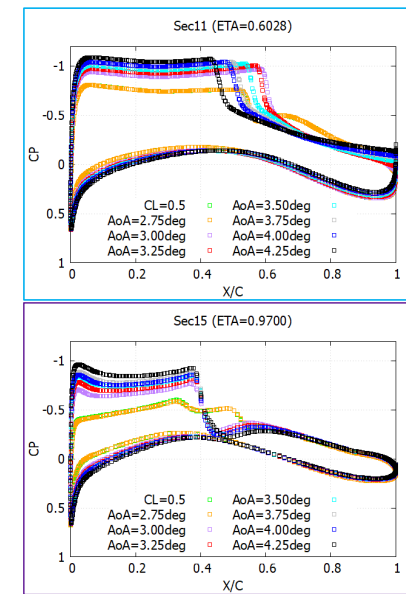
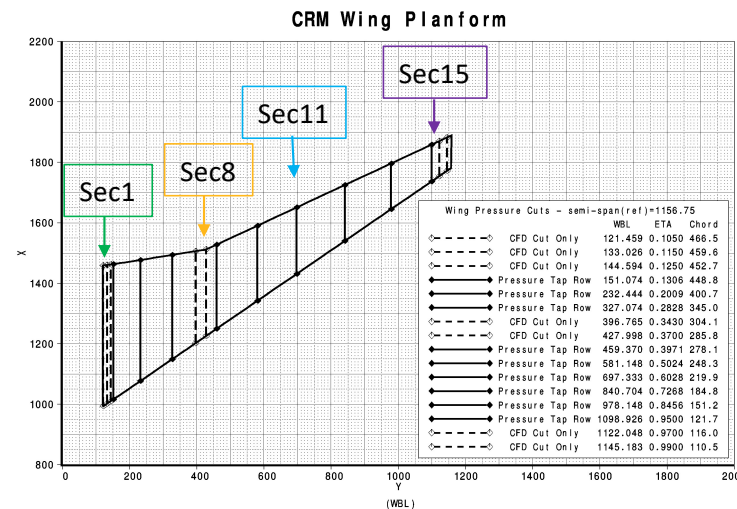
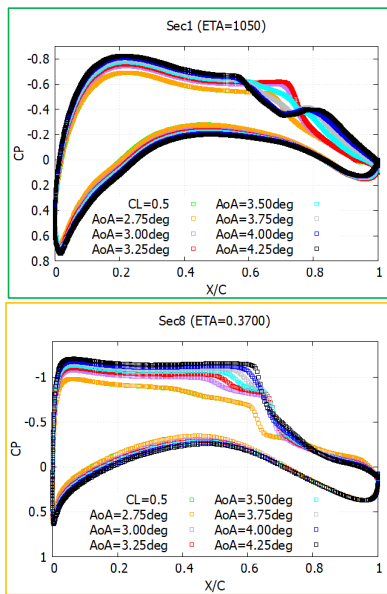
Case 2a: Pressure Coefficients

Case2a. Alpha Sweeps at Constant Re: $M = 0.85$; $Re = 20$ million; Ref. temp. = -250°F; Baseline LoQ R30 grids

- Observation:

- The wing experiences an increase in airflow speed on the suction side as the AoA increases.
- At the wing root and mid span, the shock moves downstream and then upstream .
- At section 8, Yehudi break, the shock moves downstream after an AoA of 2.75° and then stays at this position.
- At the wing tip, the shock moves upstream after an AoA of 2.75° and then stays at this position.

Pressure Coefficient (CP)

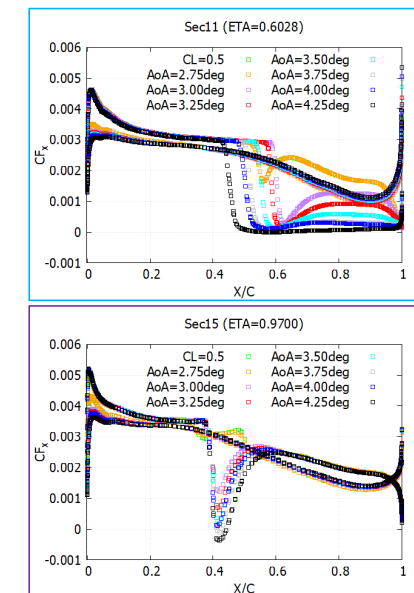
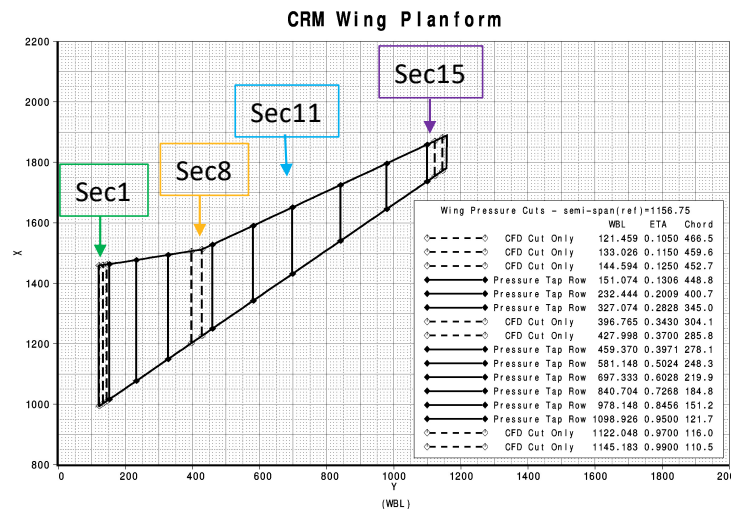
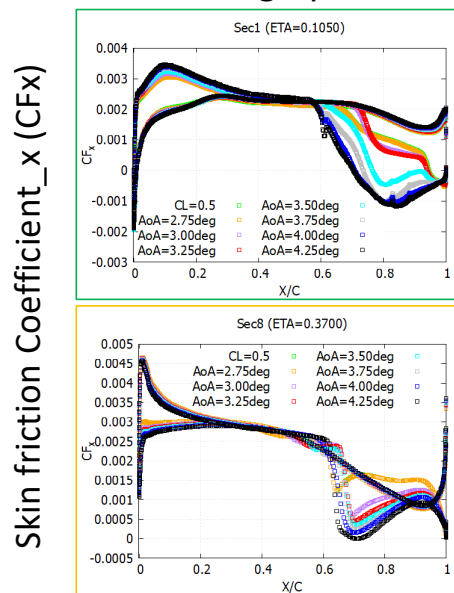


Case 2a: Skin Friction Coefficients

Case2a. Alpha Sweeps at Constant Re: $M = 0.85$; $Re = 20$ million; Ref. temp. = -250°F; Baseline LoQ R30 grids

- Observation:

- At the wing root, the separation zone increases with AoA.
- At mid-span, the separation zone increases in size with AoA, is clearly visible at an AoA of 3.0°, and reaches the Yehudi break, section 8, and the wing tip.
- At the wing tip, reverse flow appears at AoA of 4.25°.



Case 2a: Conclusion

- As the AoA increases at constant $M = 0.85$ & $Re = 20M$, the k- ω SST predicts, at the prescribed turbulence boundary conditions,
 - A pitch break between 3.0° and 3.25° which closely corresponds to the appearance of the shock-induced separation at mid-span
 - The size of each separation zone increases with AoA.
 - At wing root, the separation zone size increases and creates multiple recirculation bubbles which then merged with one another.
 - At mid-span, the shock-induced separation bubble extends beyond the Yehudi break and towards the wing tip.
- Sudden inflection in C_L vs AoA [4.0° - 4.25°] could be due to change in wing bending
- Suggestions to improve accuracy and precision:
 - Include RSM type turbulence models as secondary flows become predominant with increasing AoA
 - Perform sensitivity analysis of turbulence boundary conditions
 - Conduct extra grid convergence study at a higher AoA to verify if the medium mesh is suitable.

CFD Results

Case3. Reynolds Number Sweep at Constant CL:

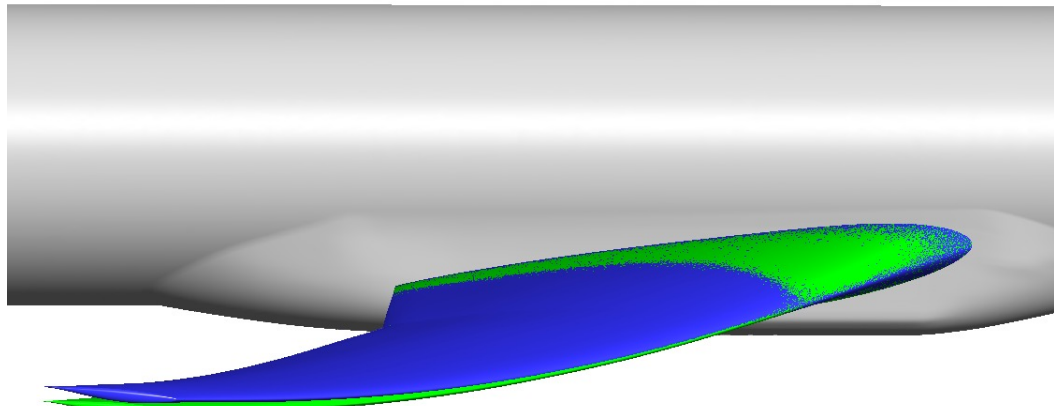
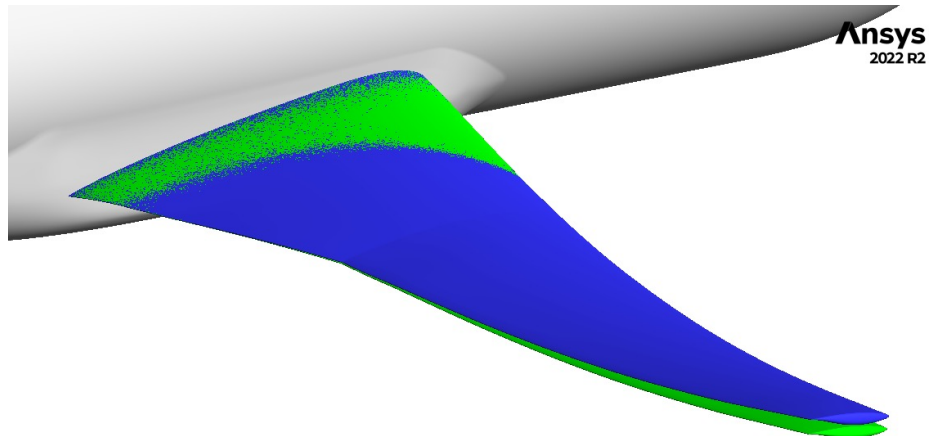
$M = 0.85$; ***fixed CL = 0.5 +/- 0.0001***; Medium grids



Case 3: Conditions and Aerodynamic Coefficients

Case3. Reynolds Number Sweep at Constant CL: $M = 0.85$; $CL=0.5$; Medium grids

Grid Level Medium	Reynolds Number	AoA (deg)	CL	CD	CM
LoQ-R5 2.50deg LoQ AE CRM Geom.	5 million	2.513	0.5000	0.02671	-0.09100
LoQ-R30 2.50deg LoQ AE CRM Geom.	20 million	2.258	0.4999	0.02339	-0.11113
HiQ-R30 2.50deg HiQ AE CRM Geom.	20 million	2.438	0.4999	0.02355	-0.09916
HiQ-R30 2.50deg HiQ AE CRM Geom.	30 million	2.380	0.5000	0.02284	-0.10298

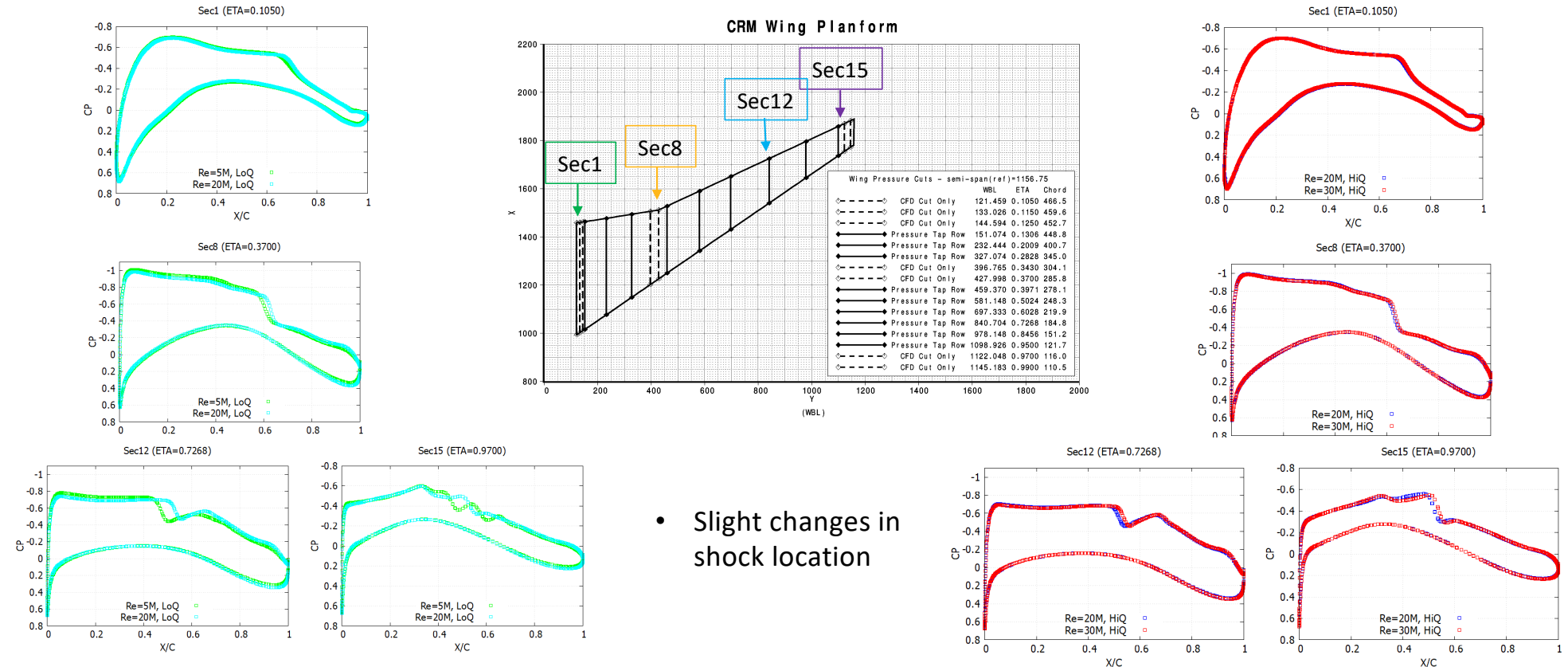


2.50deg LoQ AE CRM Geom
2.50deg HiQ AE CRM Geom

- An increase in Reynolds number decreases AoA and C_D to meet a target C_L of 0.5.

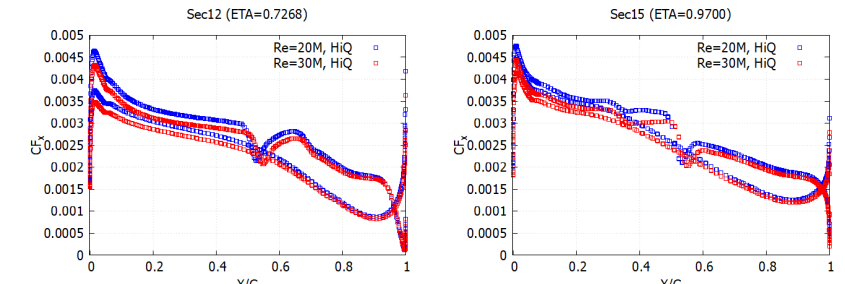
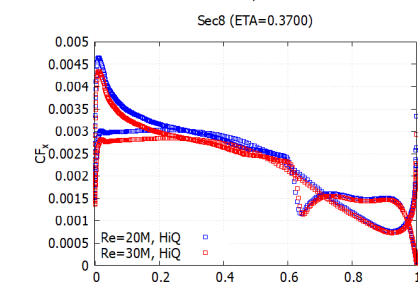
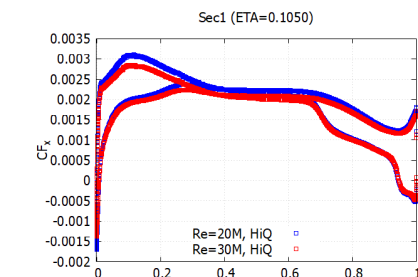
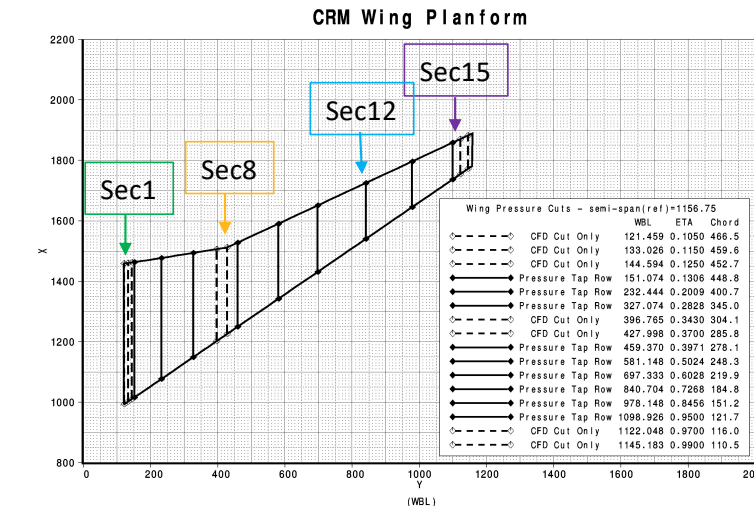
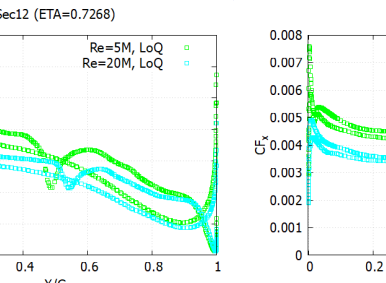
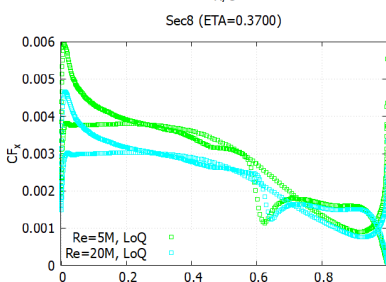
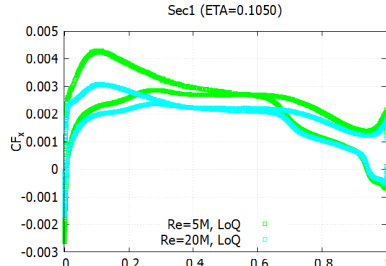
Case 3: Pressure Coefficients

Case3. Reynolds Number Sweep at Constant CL: $M = 0.85$; $CL=0.5$; Medium grids



Case 3: Skin Friction Coefficients

Case3. Reynolds Number Sweep at Constant CL: $M = 0.85$; $CL=0.5$; Medium grids



- Reduction in skin friction with increasing Reynolds

Case 3: Conclusion

Case3. Reynolds Number Sweep at Constant CL: $M = 0.85$; $CL=0.5$; Medium grids

- At a constant C_L of 0.5, the AoA and the C_D decrease as Reynolds number increases since viscous forces become less important.
- Slight changes in AoA might explain the differences in pressure coefficient distributions as well as the shock location
- Skin friction coefficients slightly change as the Reynolds number increases beyond 20M.

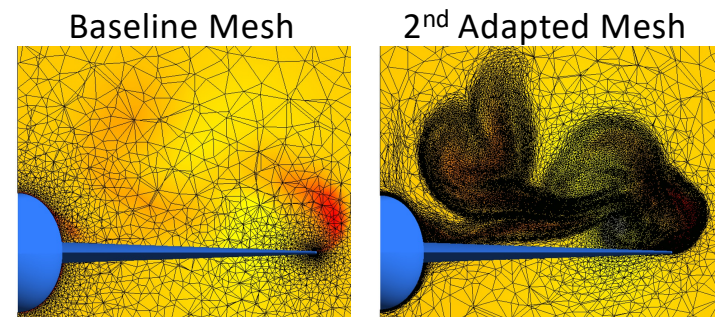
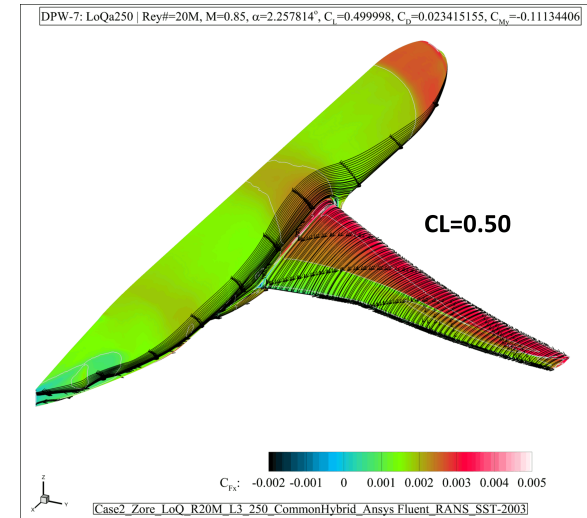


Conclusion & Outlook



Conclusion & Outlook

- This study revealed that:
 - Case 1a: Grid convergence study at constant C_L
 - Even if the aerodynamic forces barely change with mesh refinement, viscous forces on the suction side still vary between the Fine and Extra Fine meshes at the wing tip and wing root.
 - **Suggestion:** Perform grid convergence at fix AoA instead of target C_L to remove boundary condition uncertainty due to small AoA variations.
 - Case 2a: AoA sweeps at constant Re
 - As AoA increases, the separation bubbles at the junction and at mid-span increase.
 - The k- ω SST model predicts a pitch break between 3.0° and 3.25° AoA.
 - **Suggestion:** Conduct an extra grid convergence study at high AoA ($\sim 4.25^\circ$) since the airflow above the suction side of the wing largely varies (predominance of secondary flow) between $\sim 2.8^\circ$ and $\sim 4.25^\circ$.
 - Case 3: Re sweeps at constant C_L
 - AoAs prediction consistent with changes in Reynolds number at constant C_L .
- Further investigation:
 - Sensitivity of results to turbulence models and boundary conditions.
 - Sensitivity to turbulence intensity and turbulence viscosity ratios.
 - Sensitivity to Reynolds Stress turbulence models (RSM), for instance BSL-EARSM.
 - Enhance precision using anisotropic mesh adaptation with Ansys OptiGrid.



Reference: Aerodynamic and Stealth Studies of Canard-Wing Configurations at Transonic Speeds Using Ansys Fluent & Ansys HFSS SBR+